



The importance of ammonia for springtime atmospheric new particle formation and aerosol number abundance over the United States

Arshad Arjunan Nair*, Fangqun Yu, Gan Luo

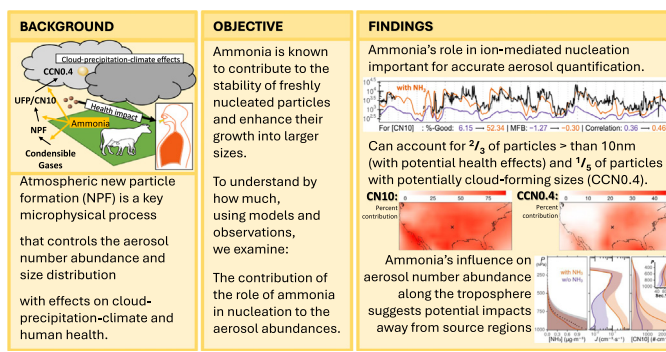
Atmospheric Sciences Research Center, State University of New York, Albany 12226, NY, USA



HIGHLIGHTS

- NH₃ crucial for observed new particle formation events and aerosol numbers in spring.
- Role of NH₃ in ion-mediated nucleation can explain 63 ± 15 % of CN10 numbers.
- Without NH₃'s participation in NPF, springtime US CCN underestimated by 16 ± 10 %.
- Measured PM₁ ammonium suggests a possible link for largest improvements in modeled CCN.
- NH₃ vertical influence across the troposphere may have impacts beyond source regions.

GRAPHICAL ABSTRACT



ARTICLE INFO

Editor: Hai Guo

Keywords:

New particle formation (NPF)
Ammonia (NH₃)
Ion-mediated nucleation (IMN)
Particle size distributions (PSD)
Aerosol number concentration ultrafine particles (UFP)

ABSTRACT

New particle formation (NPF) and subsequent growth can contribute upwards of 50 % of the global cloud condensation nuclei (CCN) budget. It is also a significant source of ultrafine aerosols (PM_{0.1}) with health implications. Ammonia (NH₃) can play a significant role in enhancing NPF and contributing to the growth of nucleated particles. Understanding these processes are vital for air quality and climate. Here, we examine the role of NH₃ in NPF and consequent effects on aerosol number concentrations (including CCN) and size distributions during springtime over the United States (US). We use the GEOS-Chem chemistry transport model coupled with the size-resolved Advanced Particle Microphysics (APM) Model. We also employ measurements of particle number size distributions, CN10 (condensation nuclei > 10 nm), CCN0.4 (CCN at 0.4 % supersaturation), and aerosol composition (SO₄, NO₃, NH₄, Organics) at the Southern Great Plains site (SGP). The impact of NH₃ in ion-mediated nucleation is the improved capturing of the occurrence of almost all springtime (March–April) NPF events observed at SGP during 2015–2020. Furthermore, this brings the magnitude and temporal variations of particle number concentrations in stronger agreement with observations; mean fractional bias for modeled CN10(CCN0.4) reducing from -1.26 to -0.27 (-0.75 to -0.54) and overall good-agreement ($|FractionalBias| < 0.6$) improving from 8.5 to 54 % (31 to 42 %). The contribution of NH₃ in new particle formation is important for springtime abundance of ultrafine aerosols (explaining 63 ± 15 % of CN10) and CCN (16 ± 10 % of CCN0.4) over the US. Our analysis shows that the deviation of CCN0.4 is strongly correlated with PM₁-NH₄⁺ deviations, suggesting the importance of improved model representation of ammonium for more accurate quantification of potential cloud forming particles.

1. Introduction

Ammonia (NH₃) plays important roles in the atmosphere due to its alkalinity and abundance (Nair and Yu, 2020). Of focus here is its role in atmospheric new particle formation (NPF) or nucleation (Kirkby et al., 2011;

* Corresponding author.

E-mail addresses: aanair@albany.edu (A.A. Nair), fyu@albany.edu (F. Yu).

Dunne et al., 2016; Yu et al., 2018), where gases condense to form clusters that undergo further growth to form secondary aerosols (Seinfeld and Pandis, 2016). While NPF does not significantly impact aerosol mass, which is dominated by larger aerosols, its largest role in determining aerosol numbers is clear (Kulmala et al., 2004; Yu and Luo, 2009; Pierce and Adams, 2009; Zhang et al., 2011). Beyond aerosol mass or composition, aerosol abundance, i.e. the number concentration of tiny particles in the atmosphere, is demonstrated to be the key aerosol property in terms of health (Kaur et al., 2007; Hoek et al., 2009; Han et al., 2016) and climate (Junge and McLaren, 1971; Fitzgerald, 1973; Dusek et al., 2006; Nair et al., 2021) impacts. Even in regions of low NH₃ concentrations, it is shown to enhance NPF rates by several hundred-fold even at tens of pptv levels. Additionally, this is typically accompanied by a regime of clean (low cloud-seeding aerosol numbers) clouds susceptible (Martin et al., 1994; Ramanathan, 2001) to the large relative changes due to secondary aerosol formation that can be enhanced by NH₃.

In typical conditions of the atmosphere, nucleation is predominantly with hydrophilic H₂SO₄ vapors (e.g., Doyle, 1961; Jaecker-Voirol and Mirelbel, 1989; Lee et al., 2019). In addition to the role of ions (Yu and Turco, 2001), the presence of cluster stabilizing species such as NH₃ is crucial to explain theoretical (Nadykto and Yu, 2007; Torpo et al., 2007) and observed (e.g., Kim et al., 1998; Ball et al., 1999; Hanson, 2002; Benson et al., 2009; Kirkby et al., 2011; Zollner et al., 2012; Froyd and Lovejoy, 2011; Glasoe et al., 2015; Schobesberger et al., 2015; Kürten et al., 2016; Duplissy et al., 2016), rates of nucleation. While amines and other organic species may also enhance H₂SO₄ nucleation (Lee et al., 2019), our focus is on NH₃ considering that it is the most abundant alkaline atmospheric gas. The ion- and ammonia-enhanced nucleation and its contribution to particle numbers have been recently investigated (Yu et al., 2020). However, there still remain uncertainties as the study was focused on the Northeastern US and for wintertime, when competing biogenic precursors are negligible. Additionally, due to the lack of cloud condensation nuclei (CCN) numbers and aerosol composition measurements, the specific contribution of NH₃ to aerosol growth (and compositions) and CCN abundance remains to be elucidated.

The objective of this study is to probe the role of ammonia in NPF and its contribution to aerosol numbers (including CCN) over the conterminous United States during springtime. This is a period when NH₃ is typically abundant (Nair and Yu, 2020) due to its higher emissions and conditions are prime for frequent observations of NPF (Lee et al., 2019). To aid our study, we also employ observations from the US Department of Energy's (DOE) Atmospheric Radiation Measurement (ARM) Southern Great Plains (SGP) Central Facility located in Lamont, Oklahoma. The SGP site was established with the mission statement of "provid[ing] the climate research community with strategically located in situ and remote-sensing observatories designed to improve the understanding and representation, in climate and earth system models, of clouds and aerosols as well as their interactions and coupling with the Earth's surface." High-quality, continuous, and simultaneous in situ measurements of particle number size distribution, [CN10], [CCN0.4], and aerosol composition in the United States are only available from the SGP site. For studying the role of NH₃ in new particle formation, the location of this site makes this an ideal test-bed: mid-latitude remote location in a region of varied atmospheric dynamical and chemical processes and in a source region of various aerosol precursors (such as NH₃ from open-lot dairies and farms and acidic precursors from anthropogenic activities). It should be noted that while NPF events are known to occur at SGP (e.g., Wang et al., 2006; Hodshire et al., 2016; Chen et al., 2018; Marinescu et al., 2019), this work represents the first such model-observation comparison study at the SGP site. The role of ammonia in nucleation is examined through a sensitivity study and with aerosol composition measurements. Considering the increasing trend and changing spatiotemporal variability of atmospheric ammonia due to increasingly stringent control of acid precursor gases (SO₂ and NO_x), this is important toward understanding the subsequent aerosol-health impacts and aerosol-cloud interactions, which are the largest source of uncertainty in climate change assessment (IPCC, 2013).

2. Data and methods

2.1. Observations at the Southern Great Plains

The US DOE ARM SGP site located in Lamont, Oklahoma (36°6'18" N, 97°9'6" W, 318 m) provides high-quality, continuous, and simultaneous in situ measurements of PNSD, [CN10], [CCN0.4], and aerosol composition that are described as follows:

2.1.1. Particle number size distribution (PNSD)

Particle number size distribution from ~3–500 nm is measured using a TSI Inc. Model 3936 Scanning Mobility Particle Spectrometer (SMPS) and is publicly available (Kuang and Ermold, 2021; Howie and Kuang, 2021). Sampled aerosol is imparted charge and differentially counted by size by exploiting the mobility of a charged particle in an electric field. Further details are available from Kuang (2016) (technical) and Knutson and Whitby (1975) (scientific). Supplementary Text S2 details the merging procedure to ensure consistency of the PNSD measured by the two instruments (nanoSMPS and regular SMPS).

2.1.2. [CN10]

Condensation nuclei of diameter greater than 10 nm (CN10) have their number concentrations measured using a TSI Inc. Model 3772 Condensation Particle Counter (CPC) and is publicly available (Salwen et al., 2010). These aerosols are counted by their optical scattering following their condensational growth by instrument modification of supersaturation. Corrections to account for inlet flow, dilution, size-dependent counting efficiency, and particle coincidence at high concentrations are applied following instrument calibrations. Further details are available in Stolzenburg and McMurry (1991).

2.1.3. [CCN0.4]

Cloud condensation nuclei (CCN) number concentrations are measured using a Droplet Measurement Technologies CCN-100/CCN-200 (CCNc) and is publicly available (Koontz and Flynn, 2022; Koontz and Uin, 2022). This instrument is a continuous-flow thermal-gradient diffusion chamber for effectively counting aerosols that can act as cloud condensation nuclei. Aerosol is drawn into a column with well-controlled and quasi-uniform centerline supersaturation. The temperature gradient and flow rate are software-controlled to vary supersaturations and obtain the CCN spectra. Just as cloud droplets form in the atmosphere, water vapor condenses onto sampled CCN to form droplets, and an Optical Particle Counter (OPC) counts and sizes these activated droplets as a function of supersaturation. Further details are available from Uin (2016) (technical) and Roberts and Nenes (2005) (scientific). Supplementary Text S3 details the approximation of [CCN0.4] when the instrument supersaturation ≠ 0.4% (Nair et al., 2021).

2.1.4. Sub-micron aerosol composition

Non-refractory sub-micron (PM₁) aerosol mass loadings and their chemical composition (Org: organics, SO₄: sulfate, NO₃: nitrate, NH₄: ammonium, and Cl: chloride) are measured using an Aerodyne Research Inc. aerosol chemical speciation monitor (ACSM; Ng et al., 2011) with technical specifications in Watson (2017) and Shilling and Levin (2021). This data is publicly available (Zawadowicz and Howie, 2022).

2.2. IASI satellite inference of NH₃

The Infrared Atmospheric Sounding Interferometer (IASI) onboard the EUMETSAT/ESA polar sun-synchronous MetOp-A satellite launched in 2006 crosses the equator at a mean local solar time of 09:30 and 21:30. This instrument measures infrared radiation from Earth in the 645–2760 cm⁻¹ spectral range, with an unapodized (apodized) resolution of ~0.25 (0.5) cm⁻¹ and noise-equivalent-change-in-temperature of 0.2–0.3 K at 280 K. It has an elliptical footprint of 12 km × 12 km (at nadir) and up to 20 km × 39 km (off nadir; 48°). We use the Standard monthly IASI/Metop-A ULB-LATMOS

ammonia (NH_3) L3 product (van Damme et al., 2017), where NH_3 columns are retrieved from measured radiance spectra via an artificial neural network, with a fixed vertical profile. The $0.01^\circ \times 0.01^\circ$ resolution monthly average global column NH_3 dataset is publicly available (<https://iasi.aeris-data.fr/>) and used in this study for model–observation comparison of vertical $[\text{NH}_3]$.

2.3. AMoN measurements of surface NH_3

In situ observations for the assessment of model simulated $[\text{NH}_3]$ are obtained from the United States Ammonia Monitoring Network (AMoN) by the National Atmospheric Deposition Program (NADP, 2017), which provides a consistent and long-term $[\text{NH}_3]$ record over North America from 2007. For the domain and period of study, data from 116 AMoN sites are used for model–observation comparison of surface $[\text{NH}_3]$. Data are biweekly averages of surface $[\text{NH}_3]$ obtained using Radiello® passive diffusion samplers. $[\text{NH}_3]$ is estimated by flow injection analysis of sonically dislodged ammonium ions from the phosphoric acid sorbent of the diffusion sampler. Further details and data access are available at <http://nadp.slh.wisc.edu/AMoN/>.

2.4. GEOS-Chem-APM model (GCAPM)

GEOS-Chem is a global 3D chemical transport model (CTM) driven by assimilated meteorological observations from the Goddard Earth Observing System (GEOS) of the NASA Global Modeling and Assimilation Office (GMAO). Several research groups develop and use this model, which contains numerous state-of-the-art modules treating emissions (van Donkelaar et al., 2008; Keller et al., 2014) and various chemical and aerosol processes (e.g., Bey et al., 2001; Evans and Jacob, 2005; Martin et al., 2003; Murray et al., 2012; Park et al., 2004; Pye and Seinfeld, 2010) for solving a variety of atmospheric composition research problems. The ISORROPIA II scheme (Fountoukis and Nenes, 2007) is used to calculate the thermodynamic equilibrium of inorganic aerosols. An improved wet scavenging scheme (Luo et al., 2019) reducing model overestimation of aerosol nitrate and ammonium is applied. Secondary organic aerosol formation and aging are based on the mechanisms developed by Pye and Seinfeld (2010) and Yu (2011). Emissions (including those of NH_3) are prescribed by the Community Emissions Data System (CEDS) inventory, with regional inventories supplanting CEDS when available. Of relevance for the domain of study are the US Environmental Protection Agency (EPA)'s National Emission Inventory (NEI) 2011 and Canada's Air Pollutant Emission Inventory (APEI). MEGAN v2.1 (Model of Emissions of Gases and Aerosols from Nature; Guenther et al. (2012)) implements biogenic emissions and GFED4 (Global Fire Emissions Database; Giglio et al. (2013)) implements biomass burning emissions in GEOS-Chem.

The present study uses GEOS-Chem 12.9.3 (International GEOS-Chem User Community, 2020) with the implementation of the Advanced Particle Microphysics (APM) package (Yu and Luo, 2009), henceforth referred to as GCAPM. The APM model has the following features of relevance toward accurate simulation of aerosol abundance: (1) 40 bins to represent secondary particles with high size resolution for the size range important for growth of nucleated particles to CCN sizes (Yu and Luo, 2009) (2) state-of-the-art Ternary Ion-Mediated Nucleation (TIMN) mechanism (Yu et al., 2018) and temperature-dependent organic nucleation parameterization (Yu et al., 2017); (3) calculation of H_2SO_4 condensation and the successive oxidation aging of secondary organic gases (SOG) and explicit kinetic condensation of low volatile SOG onto particles (Yu, 2011); (4) contributions of nitrate and ammonium via equilibrium uptake and semi-volatile organics through partitioning to particle growth considered (Yu, 2011). Aerosol number concentrations simulated by GCAPM have previously been shown to agree well with measurements (e.g., Yu and Luo, 2009).

The horizontal resolution of GCAPM in this study is $2^\circ \times 2.5^\circ$, with 47 vertical hybrid sigma-pressure layers (14 layers from surface to 2 km above the surface). The period of simulation is March–April 2015–2020. To examine the sensitivity to ammonia, cases with and without NH_3 involvement in new particle formation are constructed. The latter case is equivalent to the

binary ($\text{H}_2\text{SO}_4\text{--H}_2\text{O}$) ion-mediated nucleation (BIMN) scheme. In spring season over the study domain (North America), both observations and models (e.g., Yu et al., 2015) indicate the role of organics-mediated nucleation (Riccobono et al., 2014) to be low, which we do not present. Since the importance of ions in the nucleation process, especially for boundary layer conditions, has been well-established (e.g., Yu and Turco, 2000; Kirkby et al., 2011; Hirsikko et al., 2011), we do not present a four-way comparison additionally with Ternary Homogenous Nucleation (THN) and Binary Homogenous Nucleation (BHN). Differences between the two cases are assumed to be solely due to the lowering of formation barriers and evaporation rates (increased stabilization) of nucleated clusters by NH_3 . This role of NH_3 is not sensitive to the uncertainty of modeled $[\text{H}_2\text{SO}_4]$ considering its typical peak values at SGP ($5 \times 10^6\text{--}2.5 \times 10^7$ molecules $\cdot\text{cm}^{-3}$) during nucleation event days are a more than a factor of 10 smaller than required for binary nucleation to dominate ternary nucleation (<http://apm.asrc.albany.edu/nrc/>).

2.5. Statistical information

Kendall rank correlation coefficient (τ) quantifies the model–observation correlation and fractional bias (FB) quantifies model–observation agreement. These are more robust and intuitive statistical estimators than Pearson's r and the normalized error (Nair et al., 2019). For instance, $(1 + \tau)/(1 - \tau)$ is the ratio of concordance to discordance and $2\text{MFB}/(2 - \text{MFB}) \times 100\%$ is the percent deviation. These are defined as follows:

$$\begin{aligned}\tau &= \frac{\sum_{i=2}^n (\text{sign}(C_i^m - C_{i-1}^m))(\text{sign}(C_i^o - C_{i-1}^o))}{\sqrt{\binom{n}{2}} - \frac{1}{2}\sum_{i=1}^n t_i^m(t_i^m - 1)\sqrt{\binom{n}{2}} - \frac{1}{2}\sum_{i=1}^n t_i^o(t_i^o - 1)} \\ \text{FB} &= \frac{(C_i^m - C_i^o)}{\left(\frac{C_i^m + C_i^o}{2}\right)}; \quad \text{MFB} = \frac{1}{n} \sum_{i=1}^n \frac{(C_i^m - C_i^o)}{\left(\frac{C_i^m + C_i^o}{2}\right)}\end{aligned}$$

where n is the sample size, C is the value, t is the number of ties in the i th group of ties, and superscripts o and m denote observed and modeled values, respectively.

$$\%-\text{Good} = 100 \times \frac{1}{n} \sum_{i=1}^n (|\text{FB}(i)| \leq 0.6 \rightarrow 1)$$

%-Good is defined on the basis of the Fractional Bias (FB). It is the percentage of model-simulated values in good-agreement with measurements; corresponding to fractional bias in the range $[-0.6, 0.6]$. The interval ± 0.6 is semi-arbitrary, based on Boylan and Russell (2006) and subsequent adoption as a criteria value for evaluating model–observation agreement.

Model–observation comparisons are quantified holistically by both correlation (τ) and deviation (FB) and their relative degree of their improvement.

3. Results

$[\text{NH}_3]$, $[\text{H}_2\text{SO}_4]$, surface area of pre-existing particles, ionization rates, temperature (T) and relative humidity (RH) are key parameters determining atmospheric new particle formation (Yu et al., 2018). GCAPM-simulated values for these parameters that have significant spatial heterogeneity are examined. Fig. 1(a–d) shows the horizontal distributions of these modeled parameters over the conterminous United States domain (CONUS) with their springtime (March–April 2015–2020) average in the lower boundary layer (from surface to ~ 400 m). NH_3 shows strong spatial heterogeneity in line with its source regions: the agricultural heartland that is the US Midwest and the San Joaquin Valley in California. There is a strong east–west contrast, which is also captured by the 116 sites in the AMoN network. GCAPM-simulated $[\text{NH}_3]$ are in good agreement with these surface measurements with $\text{MFB}=0.1$ and correlation of $\tau=0.42$ in line with previous spatio-seasonal analysis over the United States (Nair et al., 2019). Typical springtime

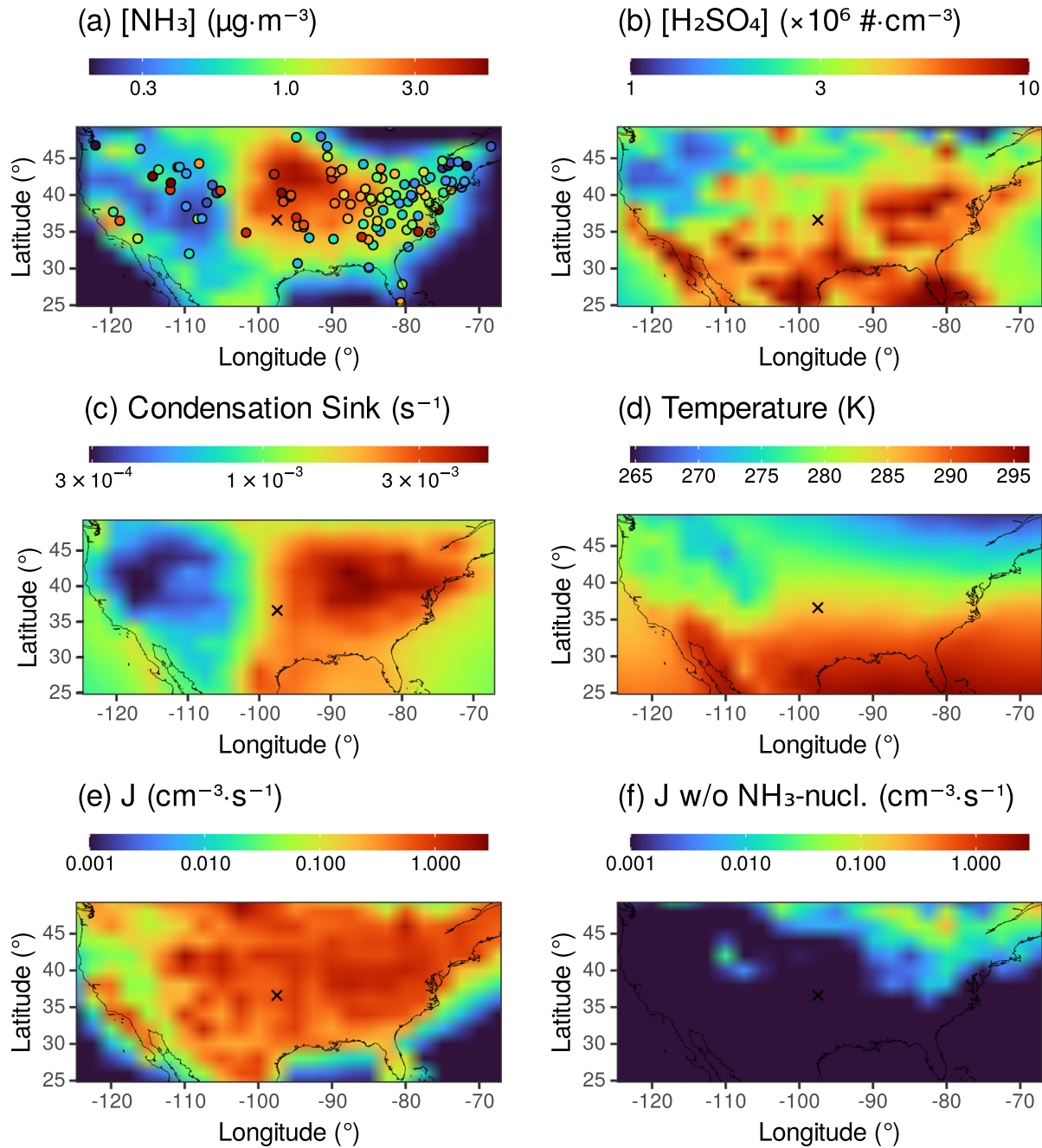


Fig. 1. New particle formation and its significant determinants. Horizontal spatial distribution of GCAPM-simulated average springtime (March–April 2015–2020) (a) $[\text{NH}_3]$, (b) $[\text{H}_2\text{SO}_4]$, (c) condensation sink (CS), (d) temperature, and nucleation rate (J) with (e) or without (f) involvement of NH_3 in new particle formation in the lower boundary layer (surface ~ 400 m, first three model layers) over the conterminous United States (CONUS). The SGP site is marked with the 'x'. In (a) observed $[\text{NH}_3]$ at AMoN sites are marked by the circles.

concentrations for $[\text{NH}_3]$ are $\sim 0.3\text{--}3 \mu\text{g}\cdot\text{m}^{-3}$ and for $[\text{H}_2\text{SO}_4]$ are $10^6\text{--}10^7 \text{ molecules}\cdot\text{cm}^{-3}$. There exists a strong east–west difference in the condensation sink, which relates to the loss rate of nucleated clusters through scavenging by pre-existing particles. GCAPM-simulated springtime nucleation rates (J) over the CONUS domain are shown in Fig. 1(e & f). The contrast in the magnitude of J in Fig. 1(e & f) is only due to the sensitivity to NH_3 . Unlike panel (e), in panel (f) the nucleation rate is for the case without the involvement of NH_3 in nucleation.

With the aid of measurements at the SGP site, we study the influence of NH_3 on nucleation rate (J), $[\text{CN}10]$, and $[\text{CCN}0.4]$ in detail. Fig. 2 shows the temporal (5-minute) evolution of the observed particle number size distribution (PNSD) at SGP in March & April 2018. New particle formation

events are frequent (30/56 days) and typically initiates in the morning and growth continues till afternoon. These events contribute to the aerosol abundance and with further growth increase $[\text{CN}10]$ and $[\text{CCN}0.4]$. Also shown are the half-hourly observed $[\text{CN}10]$ and $[\text{CCN}0.4]$ and compared with GCAPM-simulated values. Only when NH_3 is involved in the nucleation process (orange curve) does the model capture observed strong NPF events, denoted by the spike in nucleation rate. This results in significantly improved agreement of aerosol abundance with observations as these newly formed particles undergo growth processes. For $[\text{CN}10]$, which is typically dominated by the nucleation mode aerosols, the model–observation agreement increases from $7.8 \rightarrow 53\%$ with improved correlation $0.31 \rightarrow 0.43$ and correction of underestimation (MFB = $-1.3 \rightarrow -0.2$)

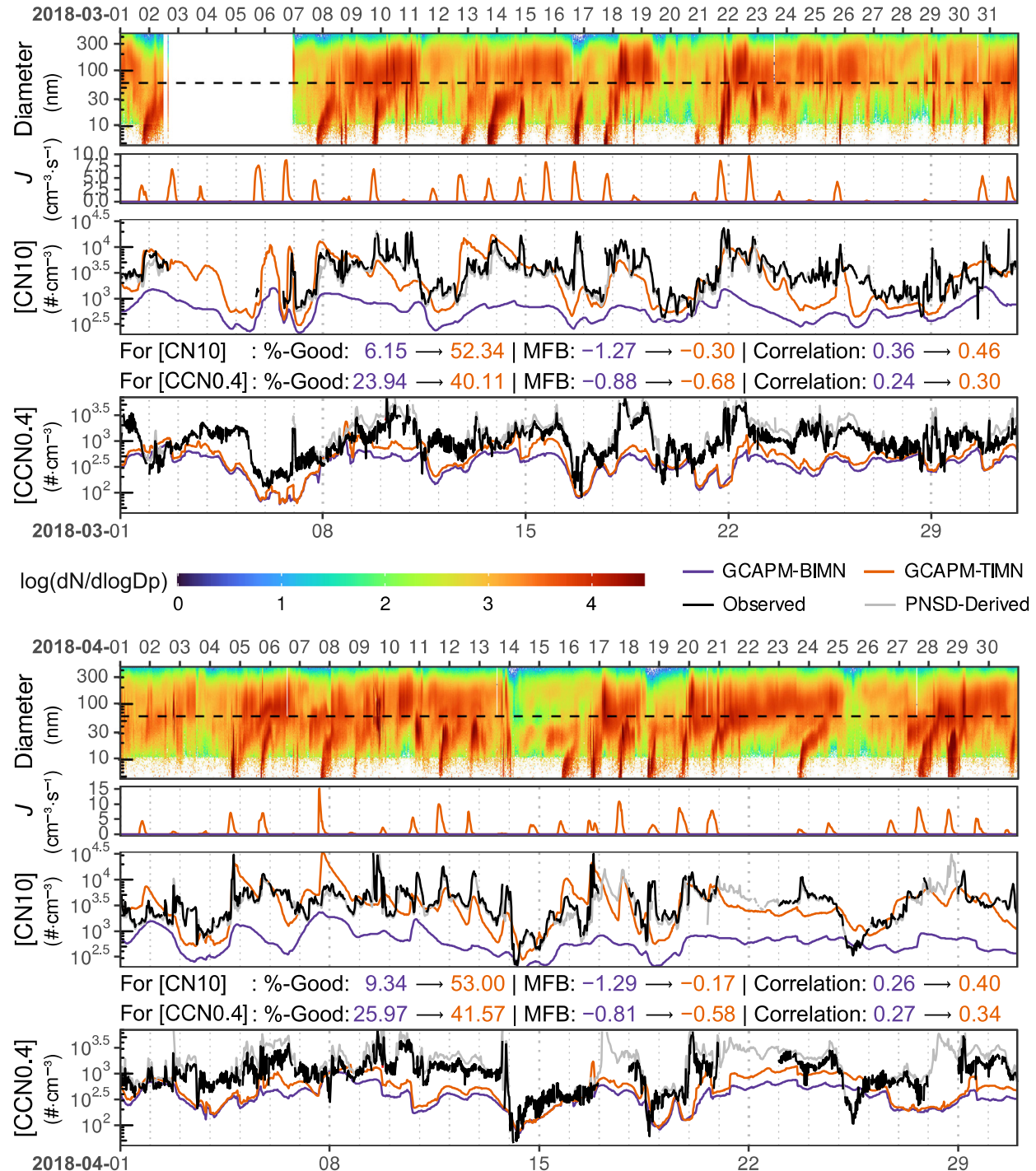


Fig. 2. Case study for the SGP site for March & April 2018. From top to bottom: observed particle number size distribution (PNSD) at SGP, occurrence of new particle formation indicated by nucleation rate (J), $[CN10]$, and $[CCN0.4]$ with (orange) or without (purple) involvement of NH_3 in new particle formation. Directly measured values are in black and PNSD-derived values in grey. Temporal resolution is half-hourly, except for PNSD at the 5-minute resolution. All times are in UTC (LT + 6).

with ternary ion-mediated nucleation. While $[CCN0.4]$ represents further grown aerosols, this too shows a higher degree of agreement in magnitude and variability (%-Good: 25 → 41, MFB = -0.9 → -0.6, and $\tau=0.26 \rightarrow 0.32$). Supplementary Figs. S5–S10 present the analysis as in Fig. 2 for the entire period of study, with the summary statistics of model–observation comparisons in Table 1. Here we have only disentangled the role of ammonia in new particle formation, i.e., the contribution of NH_3 partitioning to particle phase is considered in both cases. Owing to the strong dependence for CCN on modeled particle sizes and compositions, including the potential for condensation or reactive uptake of gases (including NH_3 among other species)

onto pre-existing aerosol (including primary particles), although the improvement in simulated $[CCN0.4]$ is significant (mean deviation reducing from 94 % to 44 %), it is not to the extent of that observed for $[CN10]$.

While NH_3 is demonstrated to be important for accurately determining the aerosol abundance, we can probe further with the aid of sub-micron aerosol composition measurements. Fig. 3 illustrates the mean fractional bias (of GCAPM w.r.t. observations) of $[CN10]$ and $[CCN0.4]$ compared to the mean fractional bias of PM_{1} speciation. For $[CN10]$, any correlation observed is weak ($\tau<0.2$). It must be noted that the apparent correlation with the organic aerosol is spurious due to instances of GCAPM low-bias

Table 1

Summary statistics for model–observation comparisons at the SGP site. For the impact of ammonia's role in springtime nucleation (Case: w NH₃) and without its participation (Case: w/o NH₃) on modeled [CN10] and [CCN0.4] as compared to their in situ measurements. *n* is the number of half-hourly measurements. Statistical metrics are %-Good: percent of model–observation with |MFB|<0.6, MFB: Mean Fractional Bias, and τ : Kendall rank correlation coefficient.

Period	Case	[CN10]				[CCN0.4]			
		%-Good	MFB	τ	<i>n</i>	%-Good	MFB	τ	<i>n</i>
Mar-15	w/o NH ₃	5.02	-1.34	0.14	717	69.32	-0.19	0.24	717
	w NH ₃	59.14	-0.25	0.35		60.81	0.12	0.23	
Apr-15	w/o NH ₃	3.49	-1.35	0.32	1406	48.65	-0.50	0.28	1406
	w NH ₃	57.33	-0.31	0.38		57.54	-0.29	0.30	
Mar-16	w/o NH ₃	0.00	-1.58	-0.03	136	81.62	-0.31	0.69	136
	w NH ₃	76.47	-0.19	0.36		88.24	-0.13	0.67	
Apr-16	w/o NH ₃				0				0
	w NH ₃								
Mar-17	w/o NH ₃	8.57	-1.27	0.31	1354	35.07	-0.68	0.20	1306
	w NH ₃	51.33	-0.38	0.41		45.94	-0.44	0.21	
Apr-17	w/o NH ₃	6.39	-1.39	0.33	1440	19.33	-0.79	0.23	1438
	w NH ₃	46.32	-0.49	0.39		31.71	-0.63	0.26	
Mar-18	w/o NH ₃	6.15	-1.27	0.36	1301	23.94	-0.88	0.24	1416
	w NH ₃	52.34	-0.30	0.46		40.11	-0.68	0.30	
Apr-18	w/o NH ₃	9.34	-1.29	0.26	1434	25.97	-0.81	0.27	1186
	w NH ₃	53.00	-0.17	0.40		41.57	-0.58	0.34	
Mar-19	w/o NH ₃	5.48	-1.21	0.43	1205	22.82	-0.94	0.26	1148
	w NH ₃	51.12	-0.22	0.43		32.84	-0.75	0.26	
Apr-19	w/o NH ₃	7.85	-1.28	0.30	1388	9.23	-1.08	0.26	1365
	w NH ₃	62.68	-0.28	0.48		28.21	-0.88	0.24	
Mar-20	w/o NH ₃	17.65	-1.07	0.28	1484	37.09	-0.65	0.15	1418
	w NH ₃	54.85	-0.10	0.39		42.03	-0.50	0.19	
Apr-20	w/o NH ₃	17.94	-1.05	0.23	708	3.95	-1.05	0.09	76
	w NH ₃	44.77	-0.13	0.29		15.79	-0.90	0.05	
Overall	w/o NH ₃	8.52	-1.26	0.30	12,573	30.93	-0.75	0.23	11,612
	w NH ₃	53.72	-0.27	0.41		41.78	-0.54	0.25	

(MFB(Organic) < -1). This indicates that the aerosol mass is insufficient to explain CN10 number concentrations. The model–observation deviations (MFBs) of [CCN0.4] and total PM₁ mass are strongly correlated ($\tau=0.52$) and mostly explained by its ammonium fraction ($\tau=0.46$). It is therefore indicative that the largest improvements in modeled [CCN0.4] may result from improvements in modeled NH₄, which is strongly dependent on accurate parameterization of NH₃ emissions, thermodynamics, and the scavenging removal of aerosols.

Fig. 4 illustrates the impact of NH₃ on modeled aerosol abundance over the United States. Shown is the lower boundary layer springtime average [CN10] and [CCN0.4]. When NH₃ participates in new particle formation, consequently higher aerosol abundances are observed. Also shown is the

surface measured value at the SGP site, with which simulated aerosol numbers are in agreement only when nucleation with the participation of NH₃ is considered. NH₃ strongly enhances aerosol abundance over its source regions, where its concentrations are highest (Fig. 5(a & c)). On average, NH₃'s role in nucleation has a significant contribution to aerosol abundance of $1450 \pm 1190 \text{ } \# \cdot \text{cm}^{-3}$ and $72 \pm 73 \text{ } \# \cdot \text{cm}^{-3}$ for [CN10] and [CCN0.4], respectively. It is important to note that here we are only explicitly teasing out the role of NH₃ in enhancing ternary ion-mediated nucleation in the lower boundary layer. In the absence of this role, aerosols can, in addition to being directly emitted (primary fraction of [CN10]: 38 ± 25% and [CCN0.4]: 64 ± 23%), have secondary origin within the LBL or transport into and mixing within the boundary layer. The enhancement of nucleation

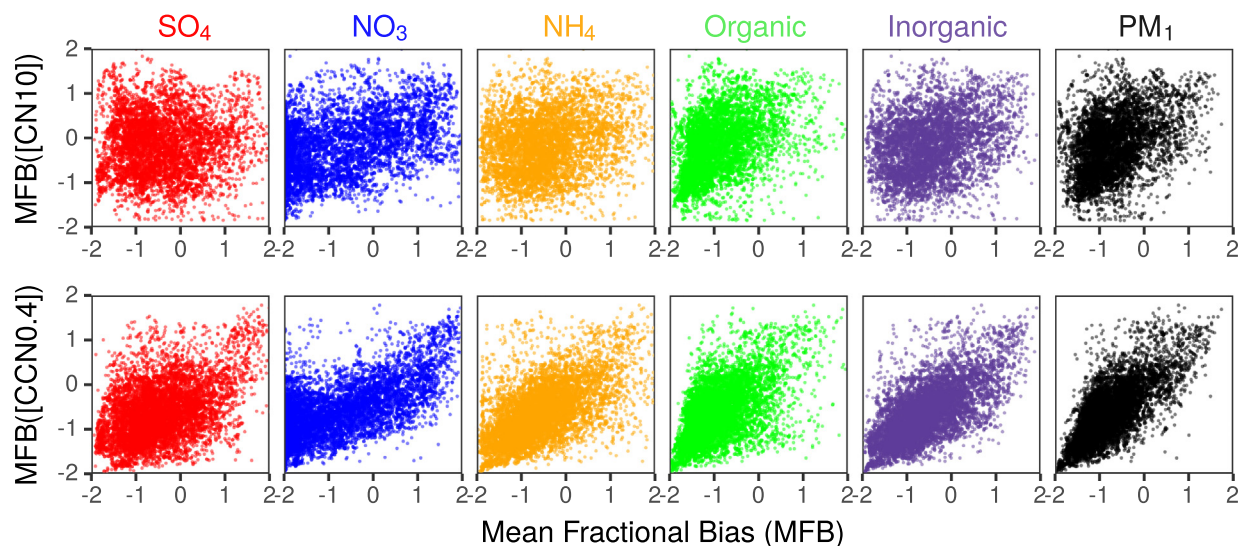


Fig. 3. PM₁ speciation impacts on aerosol abundance. Comparison of deviations in aerosol abundance (top: [CN10] and bottom: [CCN0.4]) with deviations in PM₁ speciation during the simulation period when measurements are available.

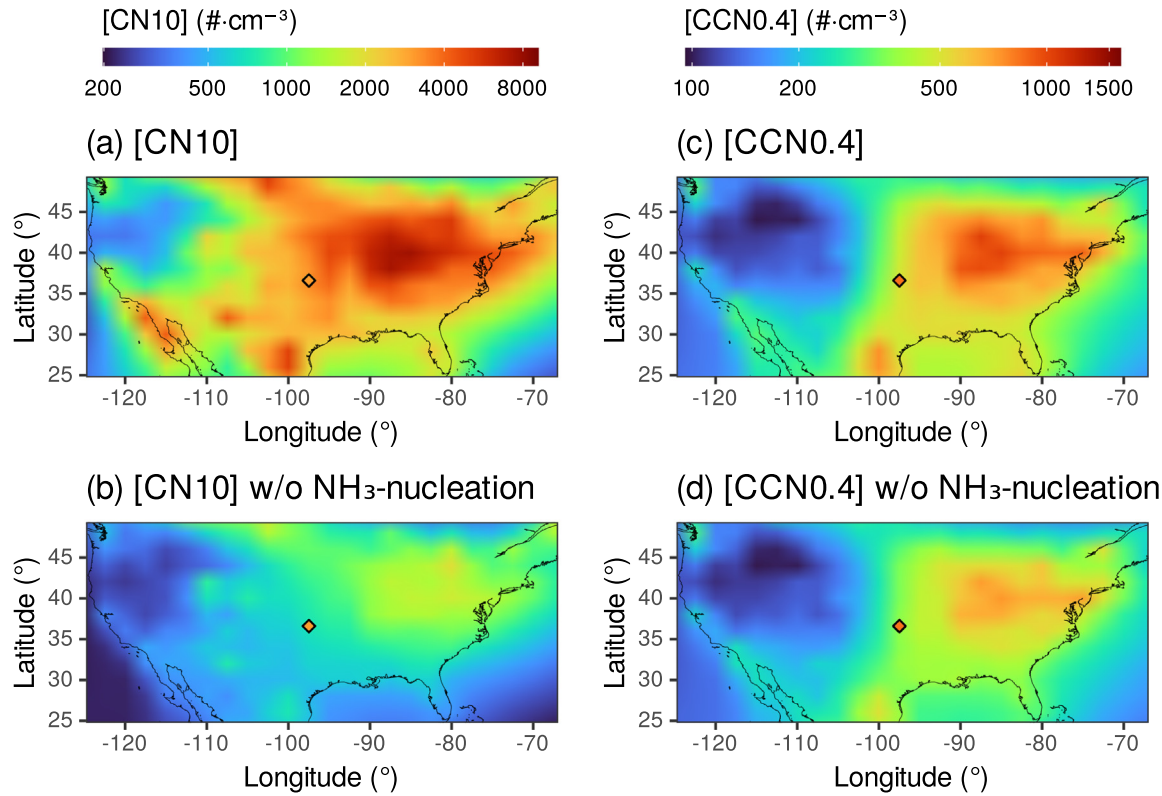


Fig. 4. Ammonia's role in the aerosol abundance over the United States. Horizontal spatial distribution of GCAPM-simulated average springtime (March–April 2015–2020) (left) [CN10] and (right) [CCN0.4] over CONUS with (top) or without (bottom) involvement of NH₃ in new particle formation in the lower boundary layer (surface ~ 400 m, first three model layers). The diamond denotes corresponding measured value at the SGP site.

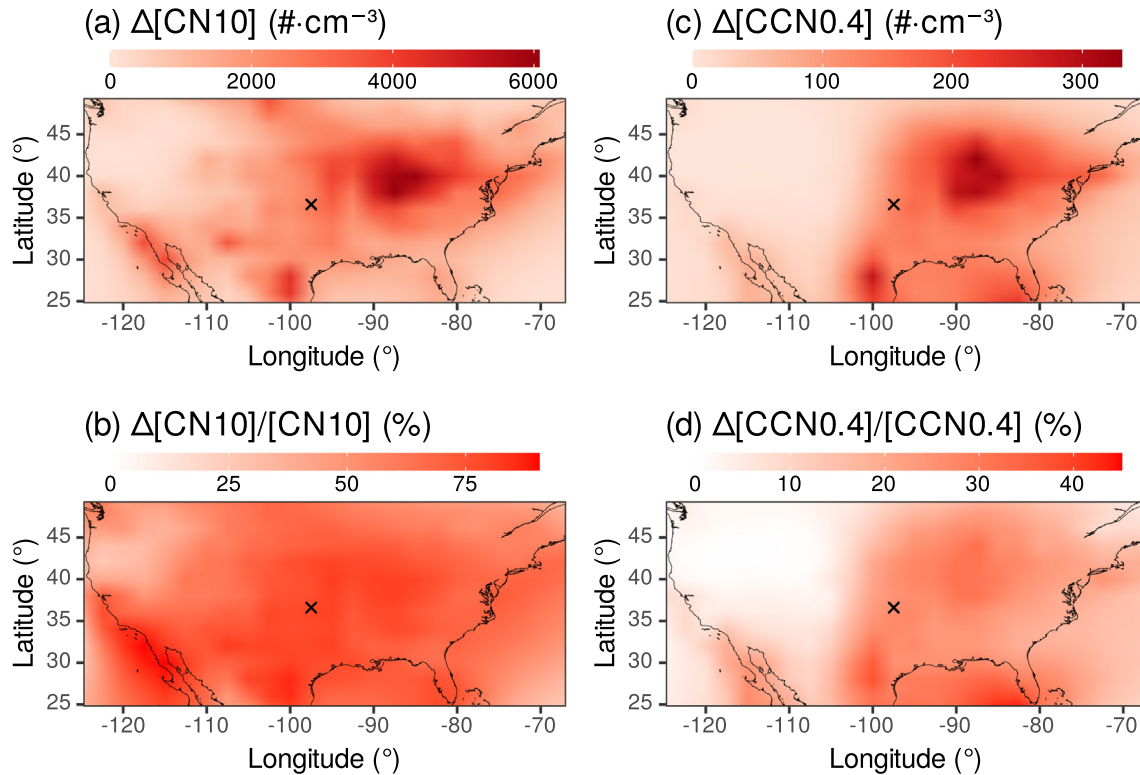


Fig. 5. Enhancement of absolute and relative aerosol abundance due to ammonia. Horizontal spatial distribution of (top) absolute and (bottom) relative differences in GCAPM-simulated average springtime (March–April 2015–2020) (left) [CN10] and (right) [CCN0.4] over CONUS with the involvement of NH₃ in new particle formation in the lower boundary layer (surface ~ 400 m, first three model layers).

by NH_3 accounts for a significant fraction of the aerosol abundance across the United States (Fig. 5(b & d)); for [CN10] it is $+63 \pm 15\%$ and for [CCN0.4] it is $+16 \pm 10\%$, with most impact over the eastern half of the US for [CCN0.4] ($+22 \pm 7.7\%$).

Over the vertical extent of the atmosphere, NH_3 is typically limited to the boundary layer ($\square 750 \text{ hPa}$ in Fig. 6(a)). Here, it significantly enhances nucleation rates (Fig. 6(b)) by over an order of magnitude on average. This enhancement consequently contributes to the aerosol abundance (Fig. 5(c & d)). However, even in the free troposphere, where $[\text{NH}_3]$ are much lower (on average $\sim 19 \times$), it can increase new particle formation rates (Fig. 6(b)). This combined with potential growth upon descent in clean (cloud-free and negligible condensation sink) conditions can have a non-trivial contribution to cloud condensation nuclei abundance.

4. Conclusions and discussions

New particle formation is a significant source of secondary aerosols and influences the number concentrations of aerosols across sizes that impact health and weather & climate (of large enough size to condense water vapor). Here, we examine the specific role of ammonia in nucleation and consequent effects on aerosol abundance for springtime over the United States, when NH_3 concentrations are the highest and meteorological conditions are suitable for NPF events. The $\text{H}_2\text{SO}_4\text{--H}_2\text{O}\text{--NH}_3$ Ternary Ion-Mediated Nucleation (TIMN) scheme constrained with thermodynamic data from quantum-chemical calculations and Cosmics Leaving OUtdoor Droplets (CLOUD) measurements captures observed NPF events during this period at the SGP site. Consequently, with aerosol growth following nucleation, the aerosol abundance is generally in good agreement with observed values. The participation of ammonia in nucleation is crucial for these model–observation agreements. Without this, over the United States, springtime [CN10] and [CCN0.4] values are largely underestimated in the boundary layer by $63 \pm 15\%$ and $16 \pm 10\%$, respectively. We find that although aerosol mass is inadequate to explain [CN10], the largest model–observation deviations in [CCN0.4] were linked to those of the submicron aerosol ammonium fraction. The variability of ammonia's effect on aerosol abundance along the tropospheric vertical extent suggest its potential impacts away from its source regions due to transport.

In this study, we have focused on the period March–April 2015–2020 and limited our analysis to the United States. This time period is chosen since springtime is a period of frequent nucleation, this is a period of increasing NH_3 abundance, and although springtime nucleation has been widely studied, the impact of TIMN (focusing on NH_3) has not been well

studied. As the present motivation is uncovering and quantifying the effect of ammonia's specific role in TIMN on the consequences for aerosol number abundances, we examine this period in detail. Observations are scarce, with only the SGP site currently having simultaneous measurements of aerosol number size distributions, concentrations, and composition. No AMoN site is in the vicinity of the SGP site and the AMoN network currently provides bi-weekly averages of surface $[\text{NH}_3]$. The satellite-inferred $[\text{NH}_3]$ along the tropospheric vertical extent assumes an a priori profile derived from the model. In addition, satellite-inferred values may deviate from the real atmospheric $[\text{NH}_3]$; the main factors are its high lower detection limit, the impact of significant cloud cover, and discontinuous measurement due to polar orbit. Although NPF is typically a regional event, the model may be too coarsely resolved for equivalence with measurements at a surface location. Regardless, analysis at a fine temporal resolution and the consequent benefit of a large sample size contributing to statistical confidence may alleviate this. While the focus of this study has been the specific role of NH_3 in new particle formation and demonstrating this to largely explain consequent aerosol abundance, regional differences may require consideration of amines (e.g., Almeida et al., 2013) and organics (e.g., Dunne et al., 2016) to close any remaining gaps between model–observations. This may especially be so for growth processes (e.g., Hodshire et al., 2016; Patel and Jiang, 2021, for SGP), which are important for freshly nucleated particles to attain (CCN) sizes relevant for aerosol–cloud interactions. In the future, more detailed examination at various locations over the globe in different seasons (not just when NH_3 is high) should shed further light on the role of ammonia in new particle formation and subsequent effects on aerosol properties with health and climate impacts.

CRediT authorship contribution statement

Arshad Arjunan Nair: Conceptualization, Methodology, Software, Validation, Formal analysis, Investigation, Resources, Data curation, Writing – original draft, Writing – review & editing, Visualization. **Fangqun Yu:** Conceptualization, Methodology, Software, Validation, Resources, Writing – original draft, Writing – review & editing, Visualization, Supervision, Project administration, Funding acquisition. **Gan Luo:** Software, Resources, Writing – original draft, Writing – review & editing.

Data availability

All datasets used in this study are publicly available as detailed in the Data and methods.

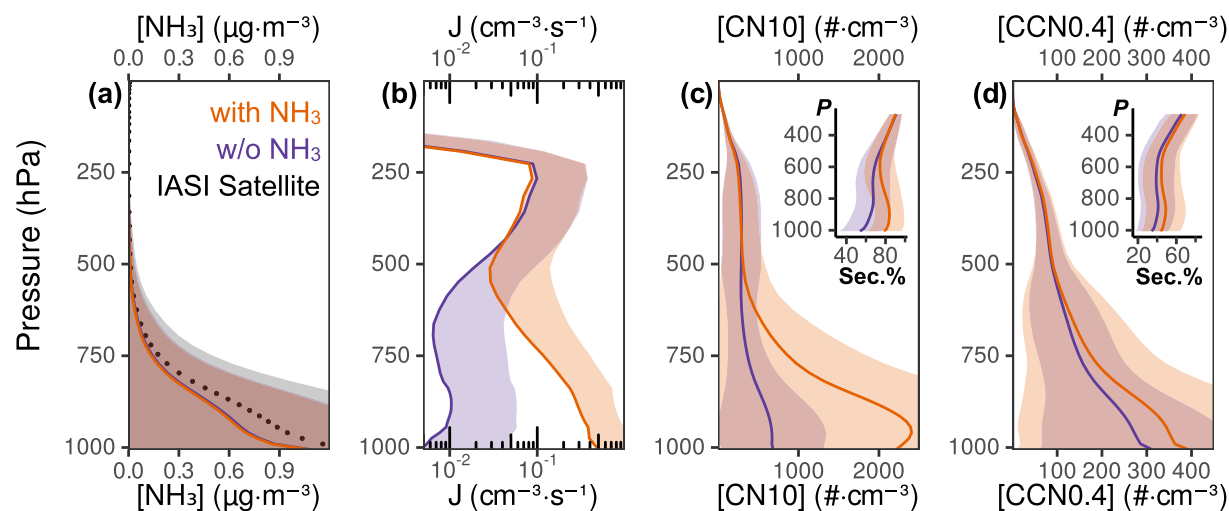


Fig. 6. Ammonia's enhancement of aerosol abundance across the atmospheric vertical extent. Vertical profile for GCAPM-simulated average springtime (March–April 2015–2020) (a) $[\text{NH}_3]$, (b) nucleation rate (J), (c) [CN10], and (d) [CCN0.4] with (orange) or without (purple) involvement of NH_3 in new particle formation. Circles in (a) denote IASI-inferred $[\text{NH}_3]$ (also see Supplementary Text S1). Indicated are mean (curve/circle) \pm standard deviation (shaded area). Inset in (c) & (d) are the secondary fraction (%) of respective aerosol number concentrations.

Declaration of competing interest

The authors declare that they have no known competing financial interests or personal relationships that could have appeared to influence the work reported in this paper.

Acknowledgments

We thank Chongai Kuang, Ashish Singh, Cynthia Salwen, Maria Anna Zawadowicz, Josh Howie, Bill Behrens, Annette Koontz, Connor Flynn, Janek Uin, and Gunnar Sernum for in situ measurements at the SGP site and Lieven Clarisse, Martin van Damme, and Pierre Coheur for IASI NH₃ measurements. Data were obtained from the Atmospheric Radiation Measurement (ARM) User Facility, a US Department of Energy (DOE) Office of Science user facility managed by the Office of Biological and Environmental Research. IASI is a joint mission of EUMETSAT and the Centre National d'Etudes Spatiales (CNES, France). The authors acknowledge the AERIS data infrastructure for providing access to the IASI data in this study and ULB-LATMOS for the development of the retrieval algorithms. Ammonia Monitoring Network (AMoN) data are available from National Atmospheric Deposition Program (NRSP-3), 2017, NADP Program Office, Illinois State Water Survey, University of Illinois, Champaign, IL 61820 (<http://nadp.slh.wisc.edu/amon/>).

This research has been supported by the National Aeronautics and Space Administration (NASA grant no. 80NSSC19K1275), Department of Energy (DOE grant no. DE-SC0022886), and the New York State Energy Research and Development Authority (NYSERDA contract no. 137487).

Appendix A. Supplementary data

Supplementary data to this article can be found online at <https://doi.org/10.1016/j.scitotenv.2022.160756>.

References

- Almeida, J., Schobesberger, S., Kürten, A., Ortega, I.K., Kupiainen-Määttä, O., Praplan, A.P., Adamov, A., Amorim, A., Bianchi, F., Breitenlechner, M., et al., 2013. Molecular understanding of sulphuric acid–amine particle nucleation in the atmosphere. *Nature* 502 (7471), 359.
- Ball, S., Hanson, D., Eisele, F., McMurry, P., 1999. Laboratory studies of particle nucleation: initial results for HSO, HO and NH vapors. *J. Geophys. Res. Atmos.* 104 (D19), 23709–23718.
- Benson, D.R., Erupe, M.E., Lee, S.-H., 2009. Laboratory-measured h₂so₄-h₂o-nh₃ ternary homogeneous nucleation rates: initial observations. *Geophys. Res. Lett.* 36 (15), L15818.
- Bey, I., Jacob, D.J., Yantosca, R.M., Logan, J.A., Field, B.D., Fiore, A.M., Li, Q., Liu, H.Y., Mickley, L.J., Schultz, M.G., 2001. Global modeling of tropospheric chemistry with assimilated meteorology: model description and evaluation. *J. Geophys. Res. Atmos.* 106 (D19), 23073–23095.
- Boylan, J.W., Russell, A.G., 2006. PM and light extinction model performance metrics, goals, and criteria for three-dimensional air quality models. *Atmos. Environ.* 40 (26), 4946–4959.
- Chen, H., Hodshire, A.L., Ortega, J., Greenberg, J., McMurry, P.H., Carlton, A.G., Pierce, J.R., Hanson, D.R., Smith, J.N., 2018. Vertically resolved concentration and liquid water content of atmospheric nanoparticles at the US DOE southern great plains site. *Atmos. Chem. Phys.* 18 (1), 311–326.
- Doyle, G.J., 1961. Self-nucleation in the sulfuric acid–water system. *J. Chem. Phys.* 35 (3), 795–799.
- Dunne, E.M., Gordon, H., Kürten, A., Almeida, J., Duplissy, J., Williamson, C., Ortega, I.K., Pringle, K.J., Adamov, A., Baltensperger, U., Barmet, P., Benduhn, F., Bianchi, F., Breitenlechner, M., Clarke, A., Curtius, J., Dommen, J., Donahue, N.M., Ehrhart, S., Flagan, R.C., Franchin, A., Guida, R., Hakala, J., Hansel, A., Heinritzi, M., Jokinen, T., Kangasluoma, J., Kirkby, J., Kulmala, M., Kupc, A., Lawler, M.J., Lehtipalo, K., Makhmutov, V., Mann, G., Mathot, S., Merikanto, J., Miettinen, P., Nenes, A., Onnela, A., Rap, A., Reddington, C.L.S., Riccobono, F., Richards, N.A.D., Rissanen, M.P., Rondo, L., Sarnela, N., Schobesberger, S., Sengupta, K., Simon, M., Sipilä, M., Smith, J.N., Stozhkov, Y., Tomé, A., Tröstl, J., Wagner, P.E., Wimmer, D., Winkler, P.M., Worsnop, D.R., Carslaw, K.S., 2016. Global atmospheric particle formation from cern cloud measurements. *Science* 354 (6316), 1119–1124.
- Duplissy, J., Merikanto, J., Franchin, A., Tsagkogeorgas, G., Kangasluoma, J., Wimmer, D., Vuollekoski, H., Schobesberger, S., Lehtipalo, K., Flagan, R.C., Brus, D., Donahue, N.M., Vehkämäki, H., Almeida, J., Amorim, A., Barmet, P., Bianchi, F., Breitenlechner, M., Dunne, E.M., Guida, R., Henschel, H., Junninen, H., Kirkby, J., Kürten, A., Kupc, A., Määttänen, A., Makhmutov, V., Mathot, S., Nieminen, T., Onnela, A., Praplan, A.P., Riccobono, F., Rondo, L., Steiner, G., Tome, A., Walther, H., Baltensperger, U., Carslaw, K.S., 2016. Effect of ions on sulfuric acid–water binary particle formation: 2. Experimental data and comparison with qc-normalized classical nucleation theory. *J. Geophys. Res. Atmos.* 121 (4), 1752–1775.
- Dusek, U., Frank, G.P., Hildebrandt, L., Curtius, J., Schneider, J., Walter, S., Chand, D., Drewnick, F., Hings, S., Jung, D., Borrmann, S., Andreae, M.O., 2006. Size matters more than chemistry for cloud-nucleating ability of aerosol particles. *Science* 312 (5778), 1375–1378.
- Evans, M., Jacob, D.J., 2005. Impact of new laboratory studies of n₂o₅ hydrolysis on global model budgets of tropospheric nitrogen oxides, ozone, and oh. *Geophys. Res. Lett.* 32 (9).
- Fitzgerald, J.W., 1973. Dependence of the supersaturation spectrum of CCN on aerosol size distribution and composition. *J. Atmos. Sci.* 30 (4), 628–634.
- Fountoukis, C., Nenes, A., 2007. ISORROPIA II: a computationally efficient thermodynamic equilibrium model for k + -ca2+ +mg2+ +nh4+ +na+ -so42- -no3- -cl- -h2o aerosols. *Atmos. Chem. Phys.* 7 (17), 4639–4659.
- Froyd, K.D., Lovejoy, E.R., 2011. Bond energies and structures of ammonia–sulfuric acid positive cluster ions. *J. Phys. Chem. A* 116 (24), 5886–5899.
- Giglio, L., Randerson, J.T., van der Werf, G.R., 2013. Analysis of daily, monthly, and annual burned area using the fourth-generation global fire emissions database (gfed4). *J. Geophys. Res. Biogeosci.* 118 (1), 317–328.
- Glasoe, W.A., Volz, K., Panta, B., Freshour, N., Bachman, R., Hanson, D.R., McMurry, P.H., Jen, C., 2015. Sulfuric acid nucleation: an experimental study of the effect of seven bases. *J. Geophys. Res. Atmos.* 120 (5), 1933–1950.
- Guenther, A.B., Jiang, X., Heald, C.L., Sakulyanontvittaya, T., Duhl, T., Emmons, L.K., Wang, X., 2012. The model of emissions of gases and aerosols from nature version 2.1 (megan2.1): an extended and updated framework for modeling biogenic emissions. *Geosci. Model Dev.* 5 (6), 1471–1492.
- Han, Y., Zhu, T., Guan, T., Zhu, Y., Liu, J., Ji, Y., Gao, S., Wang, F., Lu, H., Huang, W., 2016. Association between size-segregated particles in ambient air and acute respiratory inflammation. *Sci. Total Environ.* 565, 412–419.
- Hanson, D.R., 2002. Measurement of prenucleation molecular clusters in the NH₃, h₂so₄, h₂o system. *J. Geophys. Res.* 107 (D12).
- Hirsikko, A., Nieminen, T., Gagné, S., Lehtipalo, K., Manninen, H.E., Ehn, M., Hörrak, U., Kerminen, V.-M., Laakso, L., McMurry, P.H., Mirme, A., Mirme, S., Petäjä, T., Tammet, H., Vakkari, V., Vana, M., Kulmala, M., 2011. Atmospheric ions and nucleation: a review of observations. *Atmos. Chem. Phys.* 11 (2), 767–798.
- Hodshire, A.L., Lawler, M.J., Zhao, J., Ortega, J., Jen, C., Yli-Juuti, T., Brewer, J.F., Kodros, J.K., Barsanti, K.C., Hanson, D.R., McMurry, P.H., Smith, J.N., Pierce, J.R., 2016. Multiple new-particle growth pathways observed at the US DOE southern great plains field site. *Atmos. Chem. Phys.* 16 (14), 9321–9348.
- Hoek, G., Boogaard, H., Knol, A., de Hartog, J., Slottje, P., Ayres, J.G., Borm, P., Brunekreef, B., Donaldson, K., Forastiere, F., Holgate, S., Kreyling, W.G., Nemery, B., Pekkanen, J., Stone, V., Wichmann, H.-E., van der Sluijs, J., 2009. Concentration response functions for ultrafine particles and all-cause mortality and hospital admissions: results of a European expert panel elicitation. *Environ. Sci. Technol.* 44 (1), 476–482.
- Howie, J., Kuang, C., 2021. Scanning Mobility Particle Sizer, b1 Level. International GEOS-Chem User Community, 2020. *geoschem/geos-chem: Geos-chem 12.9.2*. IPCC, 2013. Climate Change 2013: The Physical Science Basis. Contribution of Working Group I to the Fifth Assessment Report of the Intergovernmental Panel on Climate Change. URLCambridge University Press, Cambridge, United Kingdom and New York, NY, USA. www.climatechange2013.org.
- Jaecker-Voirol, A., Mirabel, P., 1989. Heteromolecular nucleation in the sulfuric acid–water system. *Atmos. Environ.* (1967) 23 (9), 2053–2057.
- Junge, C., McLaren, E., 1971. Relationship of cloud nuclei spectra to aerosol size distribution and composition. *J. Atmos. Sci.* 28 (3), 382–390.
- Kaur, S., Nieuwenhuijsen, M., Colvile, R., 2007. Fine particulate matter and carbon monoxide exposure concentrations in urban street transport microenvironments. *Atmos. Environ.* 41 (23), 4781–4810.
- Keller, C.A., Long, M.S., Yantosca, R.M., Da Silva, A.M., Pawson, S., Jacob, D.J., 2014. Hemco v1.0: a versatile, esm-compliant component for calculating emissions in atmospheric models. *Geosci. Model Dev.* 7 (4), 1409–1417.
- Kim, T.O., Ishida, T., Adachi, M., Okuyama, K., Seinfeld, J.H., 1998. Nanometer-sized particle formation from NH₃/SO₂/h₂o/air mixtures by ionizing irradiation. *Aerosol Sci. Technol.* 29 (2), 111–125.
- Kirkby, J., Curtiss, J., Almeida, J., Dunne, E., Duplissy, J., Ehrhart, S., Franchin, A., Gagné, S., Ickes, L., Kürten, A., Kupc, A., Metzger, A., Riccobono, F., Rondo, L., Schobesberger, S., Tsagkogeorgas, G., Wimmer, D., Amorim, A., Bianchi, F., Breitenlechner, M., David, A., Dommen, J., Downard, A., Ehn, M., Flagan, R.C., Haider, S., Hansel, A., Hauser, D., Jud, W., Junninen, H., Kreissl, F., Kvashin, A., Laaksonen, A., Lehtipalo, K., Lima, J., Lovejoy, E.R., Makhmutov, V., Mathot, S., Mikkilä, J., Minginette, P., Mogo, S., Nieminen, T., Onnela, A., Pereira, P., Petäjä, T., Schnitzhofer, R., Seinfeld, J.H., Sipilä, M., Stozhkov, Y., Stratmann, F., Tomé, A., Vanhanen, J., Viisanen, Y., Vrtala, A., Wagner, P.E., Walther, H., Weingartner, E., Wex, H., Winkler, P.M., Carslaw, K.S., Worsnop, D.R., Baltensperger, U., Kulmala, M., 2011. Role of sulphuric acid, ammonia and galactic cosmic rays in atmospheric aerosol nucleation. *Nature* 476 (7361), 429–433.
- Knutson, E., Whitby, K., 1975. Aerosol classification by electric mobility: apparatus, theory, and applications. *J. Aerosol Sci.* 6 (6), 443–451.
- Koontz, A., Flynn, C., 2022. Cloud Condensation Nuclei Particle Counter (aosccn1colavg).
- Koontz, A., Uin, J., 2022. Cloud Condensation Nuclei Particle Counter (aosccn2colaavg).
- Kuang, C., 2016. TSI Model 3936 Scanning Mobility Particle Spectrometer Instrument Handbook. Tech. Rep.
- Kuang, C., Ermold, B., 2021. Aos: Scanning-mobility Particle Sizer: Nanoscale Particles.
- Kulmala, M., Vehkämäki, H., Petäjä, T., Maso, M.D., Lauri, A., Kerminen, V.-M., Birmili, W., McMurry, P., 2004. Formation and growth rates of ultrafine atmospheric particles: a review of observations. *J. Aerosol Sci.* 35 (2), 143–176.

- Kürten, A., Bianchi, F., Almeida, J., Kupiainen-Määttä, O., Dunne, E.M., Duplissy, J., Williamson, C., Barmet, P., Breitenlechner, M., Dommen, J., Donahue, N.M., Flagan, R.C., Franchin, A., Gordon, H., Hakala, J., Hansel, A., Heinritzi, M., Ickes, L., Jokinen, T., Kangashouma, J., Kim, J., Kirkby, J., Kupc, A., Lehtipalo, K., Leiminger, M., Makhmutov, V., Onnela, A., Ortega, I.K., Petäjä, T., Praplan, A.P., Riccobono, F., Rissanen, M.P., Rondo, L., Schnitzhofer, R., Schobesberger, S., Smith, J.N., Steiner, G., Stozhkov, Y., Tomé, A., Tröstl, J., Tsagkogeorgas, G., Wagner, P.E., Wimmer, D., Ye, P., Baltensperger, U., Carslaw, K., Kulmala, M., Curtius, J., 2016. Experimental particle formation rates spanning tropospheric sulfuric acid and ammonia abundances, ion production rates and temperatures. *J. Geophys. Res. Atmos.* 121 (20).
- Lee, S.-H., Gordon, H., Yu, H., Lehtipalo, K., Haley, R., Li, Y., Zhang, R., 2019. New particle formation in the atmosphere: from molecular clusters to global climate. *J. Geophys. Res. Atmos.* 124 (13), 7098–7146.
- Luo, G., Yu, F., Schwab, J., 2019. Revised treatment of wet scavenging processes dramatically improves GEOS-chem 12.0.0 simulations of surface nitric acid, nitrate, and ammonium over the United States. *Geosci. Model Dev.* 12 (8), 3439–3447.
- Marinescu, P.J., Levin, E.J.T., Collins, D., Kreidenweis, S.M., van den Heever, S.C., 2019. Quantifying aerosol size distributions and their temporal variability in the southern great plains, USA. *Atmos. Chem. Phys.* 19 (18), 11985–12006.
- Martin, G.M., Johnson, D.W., Spice, A., 1994. The measurement and parameterization of effective radius of droplets in warm stratocumulus clouds. *J. Atmos. Sci.* 51 (13), 1823–1842.
- Martin, R.V., Jacob, D.J., Yantosca, R.M., Chin, M., Ginoux, P., 2003. Global and regional decreases in tropospheric oxidants from photochemical effects of aerosols. *J. Geophys. Res. Atmos.* 108 (D3) n/a–n/a.
- Murray, L.T., Jacob, D.J., Logan, J.A., Hudman, R.C., Koshak, W.J., 2012. Optimized regional and interannual variability of lightning in a global chemical transport model constrained by lis/otd satellite data. *J. Geophys. Res. Atmos.* 117 (D20).
- NADP, 2017. Ammonia Monitoring Network (AMoN), National Atmospheric Deposition Program (NRSP-3). URL <http://nadp.sws.uiuc.edu/AMoN/>.
- Nadykto, A.B., Yu, F., 2007. Strong hydrogen bonding between atmospheric nucleation precursors and common organics. *Chem. Phys. Lett.* 435 (1–3), 14–18.
- Nair, A.A., Yu, F., 2020. Quantification of atmospheric ammonia concentrations: a review of its measurement and modeling. *Atmosphere* 11 (10), 1092.
- Nair, A.A., Yu, F., Campuzano-Jost, P., DeMott, P.J., Levin, E.J.T., Jimenez, J.L., Peischl, J., Pollack, I.B., Fredrickson, C.D., Beyersdorf, A.J., Nault, B.A., Park, M., Yun, S.S., Palm, B.B., Xu, L., Bourgeois, I., Anderson, B.E., Nenes, A., Ziemba, L.D., Moore, R.H., Lee, T., Park, T., Thompson, C.R., Flocke, F., Huey, L.G., Kim, M.J., Peng, Q., 2021. Machine learning uncovers aerosol size information from chemistry and meteorology to quantify potential cloud-forming particles. *Geophys. Res. Lett.* 48 (21), e2021GL094133.
- Nair, A.A., Yu, F., Luo, G., 2019. Spatioseasonal variations of atmospheric ammonia concentrations over the United States: comprehensive model-observation comparison. *J. Geophys. Res. Atmos.* 124 (12), 6571–6582.
- Ng, N.L., Herndon, S.C., Trimborn, A., Canagaratna, M.R., Croteau, P.L., Onasch, T.B., Sueper, D., Worsnop, D.R., Zhang, Q., Sun, Y.L., Jayne, J.T., 2011. An aerosol chemical speciation monitor (ACSM) for routine monitoring of the composition and mass concentrations of ambient aerosol. *Aerosol Sci. Technol.* 45 (7), 780–794.
- Park, R.J., Jacob, D.J., Field, B.D., Yantosca, R.M., Chin, M., 2004. Natural and transboundary pollution influences on sulfate-nitrate-ammonium aerosols in the United States: implications for policy. *J. Geophys. Res. Atmos.* 109 (D15).
- Patel, P.N., Jiang, J.H., 2021. Cloud condensation nuclei characteristics at the southern great plains site: role of particle size distribution and aerosol hygroscopicity. *Environ. Res. Commun.* 3 (7), 075002.
- Pierce, J.R., Adams, P.J., 2009. Uncertainty in global CCN concentrations from uncertain aerosol nucleation and primary emission rates. *Atmos. Chem. Phys.* 9 (4), 1339–1356.
- Pye, H.O., Seinfeld, J.H., 2010. A global perspective on aerosol from low-volatility organic compounds. *Atmos. Chem. Phys.* 10 (9), 4377–4401.
- Ramanathan, V., 2001. Aerosols, climate, and the hydrological cycle. *Science* 294 (5549), 2119–2124.
- Riccobono, F., Schobesberger, S., Scott, C.E., Dommen, J., Ortega, I.K., Rondo, L., Almeida, J., Amorim, A., Bianchi, F., Breitenlechner, M., David, A., Downard, A., Dunne, E.M., Duplissy, J., Ehrhart, S., Flagan, R.C., Franchin, A., Hansel, A., Junninen, H., Kajos, M., Keskinen, H., Kupc, A., Kürten, A., Kvashin, A.N., Laaksonen, A., Lehtipalo, K., Makhmutov, V., Mathot, S., Nieminen, T., Onnela, A., Petäjä, T., Praplan, A.P., Santos, F.D., Schallhart, S., Seinfeld, J.H., Sipilä, M., Spracklen, D.V., Stozhkov, Y., Stratmann, F., Tomé, A., Tsagkogeorgas, G., Vaattovaara, P., Viisanen, Y., Vrtala, A., Wagner, P.E., Weingartner, E., Wex, H., Wimmer, D., Carslaw, K.S., Curtius, J., Donahue, N.M., Kirkby, J., Kulmala, M., Worsnop, D.R., Baltensperger, U., 2014. Oxidation products of biogenic emissions contribute to nucleation of atmospheric particles. *Science* 344 (6185), 717–721.
- Roberts, G.C., Nenes, A., 2005. A continuous-flow streamwise thermal-gradient ccn chamber for atmospheric measurements. [Roberts and Nenes(2005)]*Aerosol. Sci. Technol.* 39 (3), 206–221.
- Salwen, C., Bullard, R., Koontz, A., Springston, S., Jefferson, A., Kuang, C., 2010. *Arm: Aos: Fine Condensation Particle Counter*.
- Schobesberger, S., Franchin, A., Bianchi, F., Rondo, L., Duplissy, J., Kürten, A., Ortega, I.K., Metzger, A., Schnitzhofer, R., Almeida, J., Amorim, A., Dommen, J., Dunne, E.M., Ehn, M., Gagné, S., Ickes, L., Junninen, H., Hansel, A., Kerminen, V.-M., Kirkby, J., Kupc, A., Laaksonen, A., Lehtipalo, K., Mathot, S., Onnela, A., Petäjä, T., Riccobono, F., Santos, F.D., Sipilä, M., Tomé, A., Tsagkogeorgas, G., Viisanen, Y., Wagner, P.E., Wimmer, D., Curtius, J., Donahue, N.M., Baltensperger, U., Kulmala, M., Worsnop, D.R., 2015. On the composition of ammonia-sulfuric-acid ion clusters during aerosol particle formation. *Atmos. Chem. Phys.* 15 (1), 55–78.
- Seinfeld, J.H., Pandis, S.N., 2016. Atmospheric chemistry and physics: from air pollution to climate change. URLWILEY. https://www.ebook.de/de/product/25599491/john_h_seinfeld_spyros_n_pandis_atmospheric_chemistry_and_physics_from_air_pollution_to_climate_change.html.
- Shilling, J.E., Levin, M.S., 2021. Aerosol chemical speciation monitor (ACSM) composition-dependent collection efficiency (CDCE) value-added product report. Tech. rep. URLDOE Office of Science Atmospheric Radiation Measurement (ARM) Program. https://www.arm.gov/publications/tech_reports/doe-sc-arm-tr-271.pdf.
- Stolzenburg, M.R., McMurry, P.H., 1991. An ultrafine aerosol condensation nucleus counter. *Aerosol Sci. Technol.* 14 (1), 48–65.
- Torpo, L., Kurtén, T., Vehkämäki, H., Laasonen, K., Sundberg, M.R., Kulmala, M., 2007. Significance of ammonia in growth of atmospheric nanoclusters. *J. Phys. Chem. A* 111 (42), 10671–10674.
- Uin, J., 2016. Cloud Condensation Nuclei Particle Counter (CCN) Instrument Handbook. Tech. Rep. DOE Office of Science Atmospheric Radiation Measurement (ARM) Program.
- van Damme, M., Whitburn, S., Clarisse, L., Clerbaux, C., Hurtmans, D., Coheur, P.-F., 2017. Version 2 of the IASI NH neural network retrieval algorithm: near-real-time and reanalyzed datasets. *Atmos. Meas. Tech.* 10 (12), 4905–4914.
- van Donkelaar, A., Martin, R.V., Leaitch, W.R., Macdonald, A., Walker, T., Streets, D.G., Zhang, Q., Dunlea, E.J., Jimenez, J.L., Dibb, J.E., et al., 2008. Analysis of aircraft and satellite measurements from the intercontinental chemical transport experiment (intex-b) to quantify long-range transport of east asian sulfur to Canada. *Atmos. Chem. Phys.* 8 (11), 2999–3014.
- Wang, J., Collins, D., Covert, D., Elleman, R., Ferrare, R.A., Gasparini, R., Jonsson, H., Ogren, J., Sheridan, P., Tsay, S.-C., 2006. Temporal variation of aerosol properties at a rural continental site and study of aerosol evolution through growth law analysis. *J. Geophys. Res.* 111 (D18).
- Watson, T.B., 2017. Aerosol Chemical Speciation Monitor (ACSM) Instrument Handbook. Tech. Rep. DOE Office of Science Atmospheric Radiation Measurement (ARM) Program.
- Yu, F., 2011. A secondary organic aerosol formation model considering successive oxidation aging and kinetic condensation of organic compounds: global scale implications. *Atmos. Chem. Phys.* 11 (3), 1083–1099.
- Yu, F., Luo, G., 2009. Simulation of particle size distribution with a global aerosol model: contribution of nucleation to aerosol and CCN number concentrations. *Atmos. Chem. Phys.* 9 (20), 7691–7710.
- Yu, F., Luo, G., Nadykto, A.B., Herb, J., 2017. Impact of temperature dependence on the possible contribution of organics to new particle formation in the atmosphere. *Atmos. Chem. Phys.* 17 (8), 4997–5005.
- Yu, F., Luo, G., Nair, A.A., Schwab, J.J., Sherman, J.P., Zhang, Y., 2020. Wintertime new particle formation and its contribution to cloud condensation nuclei in the northeastern United States. *Atmos. Chem. Phys.* 20 (4), 2591–2601.
- Yu, F., Luo, G., Pryor, S.C., Pillai, P.R., Lee, S.H., Ortega, J., Schwab, J.J., Hallar, A.G., Leaitch, W.R., Aneja, V.P., Smith, J.N., Walker, J.T., Hogrefe, O., Demerjian, K.L., 2015. Spring and summer contrast in new particle formation over nine forest areas in north america. *Atmos. Chem. Phys.* 15 (24), 13993–14003.
- Yu, F., Nadykto, A.B., Herb, J., Luo, G., Nazarenko, K.M., Uvarova, L.A., 2018. H₂SO₄-H₂O-NH₃ ternary ion-mediated nucleation (TIMN): kinetic-based model and comparison with CLOUD measurements. *Atmos. Chem. Phys.* 18 (23), 17451–17474.
- Yu, F., Turco, R.P., 2000. Ultrafine aerosol formation via ion-mediated nucleation. *Geophys. Res. Lett.* 27 (6), 883–886.
- Yu, F., Turco, R.P., 2001. From molecular clusters to nanoparticles: role of ambient ionization in tropospheric aerosol formation. *J. Geophys. Res. Atmos.* 106 (D5), 4797–4814.
- Zawadowicz, M., Howie, J., 2022. Acsm, Corrected for Composition-dependent Collection Efficiency (acsmcdce).
- Zhang, R., Khalizov, A., Wang, L., Hu, M., Xu, W., 2011. Nucleation and growth of nanoparticles in the atmosphere. *Chem. Rev.* 112 (3), 1957–2011.
- Zollner, J.H., Glasoe, W.A., Panta, B., Carlson, K.K., McMurry, P.H., Hanson, D.R., 2012. Sulfuric acid nucleation: power dependencies, variation with relative humidity, and effect of bases. *Atmos. Chem. Phys.* 12 (10), 4399–4411.